

# Evolution of the Peroxide-Induced Degradation of Polypropylene Along a Twin-Screw Extruder: Experimental Data and Theoretical Predictions

F. Berzin, <sup>1</sup> B. Vergnes, <sup>2</sup> S. V. Canevarolo,  
<sup>1</sup> A. V. Machado, <sup>1</sup> J. A. Covas <sup>4</sup>

<sup>1</sup> Centre d'Etudes et de Recherches en Matériaux et Emballages/Ecole Supérieure d'Ingénieurs en Emballage et Conditionnement, BP 1029, 51686 Reims Cedex 2, France

<sup>2</sup> Centre de Mise en Forme des Matériaux/Unité Mixte de Recherche/Centre National de la Recherche Scientifique, Ecole des Mines de Paris, 7635, BP 207, 06904 Sophia-Antipolis Cedex, France

<sup>3</sup> Department of Materials Engineering, Universidade Federal de São Carlos, São Carlos, Brazil

<sup>4</sup> Institute of Polymers and Composites, Department of Polymer Engineering, University of Minho, 4800 Guimarães, Portugal

## Abstract

This article reports an experimental and theoretical study of the peroxide-induced degradation of polypropylene in a corotating twin-screw extruder. Experiments were performed with different peroxide concentrations and different operating conditions. The evolution of the chemical reaction along the extruder was monitored with specific sampling devices. Material changes were characterized by rheological measurements and via the determination of the molecular weights of samples collected at the same locations. The theoretical

results were obtained with a model that coupled the interactions between flow conditions encountered in the extruder, the kinetics of the reaction, and

Key words: degradation; extrusion; modeling; poly(propylene) (PP)

## INTRODUCTION

Polypropylene (PP) polymerized with conventional Ziegler-Natta catalyst systems exhibits a high molecular weight (MW) and a broad molecular weight distribution (MWD) and, consequently, high viscosity and elasticity. To improve the processability of the material and to create grades with specific rheological behavior, MW and MWD can be tailored in a postreactor operation by different degradation methods.<sup>1-3</sup> The reactive process, in which PP is modified by means of organic peroxide initiated scission, yielding PP with lower MW and narrower MWD, is one of the most popular routes. It is generally accepted that PP degradation follows a series of free-radical reactions: peroxide decomposition, hydrogen abstraction, chain scission, and termination.<sup>3,4</sup> As a result of these molecular changes, the viscoelastic behavior of the polymer is deeply changed.<sup>1-3,5</sup>

Because reactive degradation is a straightforward and cost-effective approach to producing PP with controlled rheological properties (its popularity remains despite the availability of the competing metallocene catalyst technology), it has induced abundant reports in the open literature.<sup>6</sup> Initially, several authors proposed general kinetic models that were able to predict the relationship between the initiator concentration and MW and MWD of degraded PP extrudates.<sup>7-10</sup> Later, these models were coupled to descriptions of flow in processing equipment. For example, Tzoganakis and coworkers<sup>9,10</sup> and Pabedinskas et al.<sup>11</sup> combined kinetic models of the peroxideinduced PP degradation reaction with flow in singlescrew extruders. Kim and White<sup>12</sup> and, more recently, Berzin et al.<sup>13</sup> predicted MW changes along twin-screw extruders. In particular, these last authors considered the interactions occurring between flow in the extruder, reaction kinetics, and viscosity changes and their effect on the evolution of MW along the extruder. Unfortunately, the experimental validation of this theoretical approach was limited to measurements of MW on the extrudates.

Given the practical importance of the topic, this article aims at ascertaining the value of the predictions produced by Berzin et al.<sup>13</sup> for the evolution of PP's

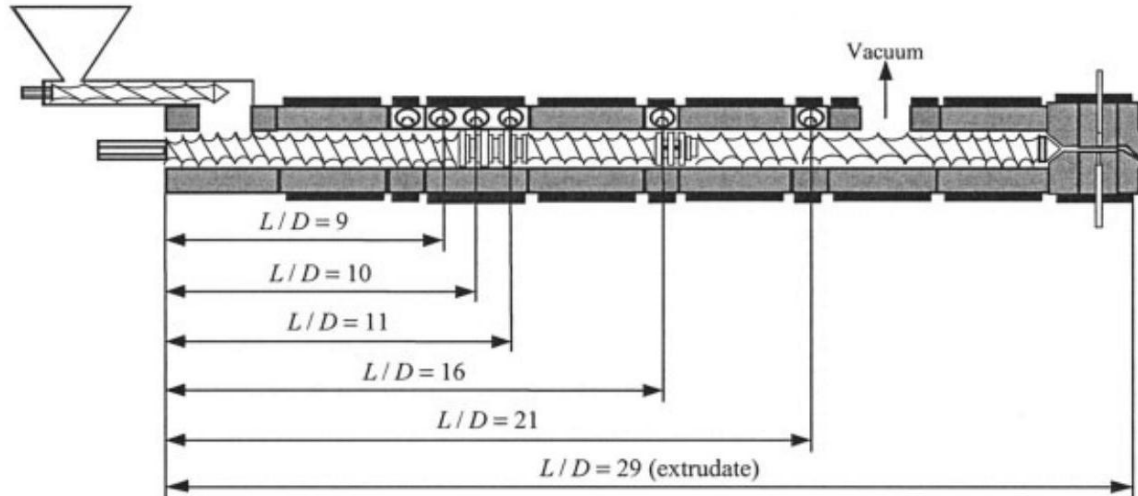


Figure 1 Screw profile and sampling locations.

MW along the axis of a corotating twin-screw extruder. For this purpose, we made use of sampling devices inserted along the extruder's barrel,<sup>14</sup> which provided the capacity of collecting 1 – 2 g of the polymer within 1-2 s. These samples were characterized in terms of their MW, MWD, and rheological behavior. Experiments with different peroxide concentrations and under various processing conditions were carried out.

## THEORETICAL MODELING

The degradation reaction was simulated with a onedimensional global model (Ludovic software, Saint Etienne, France) of polymer flow in corotating, selfwiping, twin-screw extruders. The main flow parameters (temperature, pressure, shear rate, viscosity, residence time, etc.) were calculated along the screws, from the hopper to the die exit. These computations were performed separately for each type of screw element (partially or totally filled right-handed screw elements, left-handed screw elements, and blocks of kneading disks) and for the die components. A detailed description can be found elsewhere.<sup>15</sup>

For the screw elements, the pressure/flow rate relationships were determined with the channel section assumed to be rectangular, with a constant width. It has been shown that the results yielded by this approximate one-dimensional method agree fairly well with those of a full two-dimensional computation in the usual range of feed rate variations.<sup>15</sup>

In the case of the kneading disks, only the peripheral flow was taken into consideration. Because of the disk geometry and the relative barrel-disk velocity, this flow was characterized by a pressure peak located just before the disk tip. Because the tips of adjacent disks were staggered, so were the local pressure profiles, and this created an axial pressure gradient parallel to the screw axis and pushing the material in the axial direction.

The preceding basic models were linked together to obtain a global description of the flow field along the extruder. Melting was included either by the insertion of a specific model<sup>16</sup> or by the assumption that it was an instantaneous process that took place just before the most upstream restrictive element of the screw profile. From then onward, the melt flow developed in fully or partially filled screw channels, depending on the local geometry

and flow conditions. In fact, because this type of extruder was operated starve-fed, the filling ratio of the system was not known a priori. Thus, computations had to start from the die and proceed backwards. However, because the melt exit temperature was also unknown, an iterative procedure was used.

The kinetic reaction model (see Berzin et al. <sup>13</sup> for a detailed description) was based on a reaction mechanism that comprised the following steps: free-radical initiation, hydrogen abstraction and chain  $\beta$  scission, intermolecular chain transfer, thermal degradation, and termination by disproportionation. The modeling of the reaction required knowledge of local residence times and temperatures at each screw element (for a more thorough presentation of the methodology, see Berzin et al. <sup>13</sup>). For a filled subelement, the former was estimated from the ratio between the volume occupied by the molten polymer and the total flow rate. The average temperature was determined from a local thermal balance, which included the dissipated power and the heat transfer toward barrel and screws.

As shown previously, because the screws were starve-fed, flow modeling proceeded from the die toward the hopper, as the locations at which polymer pressurization began were unknown. However, the calculation of the chemical reaction evolution along the screw had to be carried out in the opposite direction because neither the final reaction rate nor the global residence time in the extruder was known. Therefore, the calculations were initiated at the point specified by the user, in this case the beginning of the

TABLE 1  
Screw Profile from Hopper to Die

Length (mm)	120	120	300	600	900	1200	3000	2250	600	600	300	1200	600	600
Pitch (mm)	45	30	30	20	KB-60	30	KB-90	KB-60	45	30	-30	60	30	20

KB-60 indicates a block of kneading discs (each 7.5 mm thick) with a staggering angle of  $-60^\circ$ . A negative pitch indicates a left-handed element. KB-90 is a block of kneading disks with a staggering angle of  $90^\circ$ . Coupling between the chemical reaction and the thermomechanical parameters was implemented as follows (assuming that changes in viscosity due to the chemical reaction did not modify significantly the local filling ratios):

- A first calculation was performed without any coupling, with the rheological and physical properties of the virgin material (i.e., PP without peroxide). During this backward calculation, the points at which the polymer pressurization began were identified.
- A second calculation was done in the downstream direction, taking into account the interactions between the reaction conversion rate, the rheological changes, and the flow parameters.

# EXPERIMENTAL

## Materials

A commercial PP homopolymer (Stamylan P12E62, DSM, Heerlen, The Netherlands), with a melt flow index of 0.8 g/10 min(230°C/21.6 N), was selected for this work. The peroxide used as an initiator for the degradation reactions was 2,5-bis(tert-butylperoxy)-2,5-dimethylhexane (DHBP; Trigonox 101, Akzo Nobel, Milford, MA). The half-life of the peroxide at 200 and 220°C was 6.1 and 1.2 s, respectively (the values were calculated with data provided by the manufacturer). PP had an initial weight-average molecular weight ( $M_w$ ) of 1,194,400 g/mol and a polydispersity index [weight-average molecular weight/number-average molecular weight ( $M_w/M_n$ )] of 2.9.

## Processing

PP was tumble-mixed with the peroxide (in powder form) and processed in a Leistritz LSM 30-34 laboratory, modular, intermeshing, corotating, twin-screw extruder (Fig. 1). The screw profile contained a series of conveying elements, separated by three mixing zones, consisting of staggered kneading disks and a left-handed element (the detailed screw profile is presented in Table I). The first block of the kneading discs ensured the melting of PP and the homogenization of the PP/peroxide mixture. The left-handed element created a plug of material upstream of the venting port, at which any eventual residual peroxide was removed by a vacuum pump. The samples for subsequent offline characterization were quickly collected along the extruder axis with sampling devices (see Machado et al. <sup>14</sup> for details) and were immediately quenched in liquid nitrogen to avoid further reaction. The location of these devices (identified in Fig. 1) matched the sections of the screws working fully filled, at which significant thermomechanical stresses developed and, consequently, a significant evolution in PP degradation was anticipated.

The melting temperature was also measured at the sampling ports with a preheated needle of a fastresponse thermocouple stuck into the nut-shaped volume of the freshly collected material.

The operating conditions and peroxide concentrations are shown in Table II. The flow rate was kept constant at 2.3 kg/h, as guaranteed by a K-TRON gravimetric feeder (Gelnhausen, Germany). Previous work has shown that the PP degradation rate follows closely the rate of peroxide decomposition. <sup>4</sup> Because the latter is mainly dictated by temperature, low screw speeds were selected to minimize viscous dissipation. Trials 1 and 2 allowed us to check the influence of the peroxide concentration, whereas trials 1 and 3 and trials 1 and 4 did the same for the screw speed and barrel temperature, respectively. Each trial was also carried out under the same conditions but in the absence of peroxide to define reference conditions.

## Material characterization

Size exclusion chromatography (gel permeation chromatography)

The MW and MWD values of the various samples made available were measured in a Waters GPC 150

TABLE  
Operating Conditions and Peroxide Concentration

II

Trial	Barrel set temperature (°C)	Screw speed (rpm)	Peroxide concentration (phr or wt %)
1	200	75	0.05
2	200	75	0.10
3	200	15	0.05
4	220	75	0.05

Values of $M_n$ , $M_w$ , and $M_w/M_n$ Along the Screws															
Temperature (°C)/screw speed (rpm)/peroxide (phr)	$L/D = 9$			$L/D = 10$			$L/D = 11$			$L/D = 16$			$L/D = 29$ (extrudate)		
	$M_n$	$M_w/M_n$		$M_n$	$M_w/M_n$		$M_n$	$M_w/M_n$		$M_n$	$M_w/M_n$		$M_n$	$M_w/M_n$	
200/75/0.05	371,010	985,485	2.7	315,630	777,860	2.5	298,800	699,346	2.3	281,850	632,000	2.2	219,570	472,600	2.2
200/75/0.10	396,340	1,164,710	2.9	-	-	-	214,970	473,600	2.2	204,550	427,300	2.1	-	-	-

200 /15/ 0.0 5	3 7 6, 7 5 0	1, 05 3, 00 0	2 . 8	3 4 6, 0 8 0	9 0 5, 0 0	2 . 6	2 8 3, 2 3 0	6 4 6, 2 4 0	2 . 3	2 8 3, 13 0	6 3 9, 2 3 0	2 . 3	2 51 ,7 5 0	5 6 7, 5 0 0	2 . 3
220 /75 /0. 05	3 7 5, 8 0 0	1, 01 7, 43 0	2 . 7	3 2 0, 6 2 0	81 0, 0 0 0	2 . 5	-	-	-	3 5 0, 31 5	8 4 4, 0 5 0	2 . 4	3 3 7, 5 5 0	8 3 2, 8 4 0	2 . 4

CV chromatograph (Milford, MA), with a refractiveindex detector and three Waters Styragel HT columns with a 10 –  $\mu\text{m}$  particle size, able to separate samples with MWs in the range  $10^2$  to  $10^6$  g/mol. The samples were solubilized at 0.1 phr in 1,2,4-trichlorobenzene at  $140^\circ\text{C}$  and pumped at a flow rate of 1 mL/min. Calibration curves were obtained with 12 monodisperse polystyrene standards ranging from 480 to  $10^6$  g/mol. MW and MWD were determined with Millennium 2010 software (Waters, Milford, MA), with manual adjustment of the baseline. The data are presented in Table III.

## Rheology

The rheological characterization of the homopolymer and modified samples was performed on a TA Instruments Weissenberg rheometer (Gelnhausen, Germany), with parallel-plate geometry (diameter = 40 mm) with a 1.80 – mm gap. The nut-shaped samples collected from the extruder were compression-molded for 10 min at  $200^\circ\text{C}$  under a pressure of 30 tons into discs 4 cm in diameter and 2 mm thick. Frequency sweeps (from  $4 \cdot 10^{-3}$  to 40 Hz) at 180, 200, and  $220^\circ\text{C}$  were carried out. To maintain the material behavior within the linear viscoelastic domain, the applied strain was 0.01. Previous work<sup>4</sup> showed that under these experimental conditions, no significant evolution in peroxide degradation would be detected.

## RESULTS AND DISCUSSION

### Experimental results

We first consider the experimental data obtained. As shown in Table IV, the melting temperatures could be both below (in the first part of the screws) and above the set temperatures. As an example, Figure 2 presents the temperature evolution for 15 and 75 rpm, the other conditions being identical (trials 1 and 3). As expected, the low screw speed range tested induced modest viscous dissipation, the maximum temperatures reached being less than  $10^\circ\text{C}$  above the set value. Starting from 175 to  $180^\circ\text{C}$  at the melting section (upstream of the first kneading block), the temperature increased rapidly and reached the barrel temperature (or slightly above, as in the case of 75 rpm). The left-handed element (third

mixing zone) did not induce a temperature rise because of the low speeds and the very low viscosity of degraded PP.

Figure 3 depicts the evolution of MW along the screws for trial 1. Figure 3(a) shows a progressive disappearance of the higher MW species and a reduction of the breadth of the distribution. Figure 3(b) shows more explicitly that the decrease in the average MW was very rapid and tended to stabilize at the second kneading block. The change in the polydispersity followed closely that in MW. Here, the polydispersity index varied from 2.9 (virgin PP) to 2.15 (extrudate).

The data obtained from offline rheological measurements of the samples collected (trial 1) are presented in Figure 4 in terms of both the storage modulus ( $G'$ ) [Fig. 4(a)] and the complex viscosity [ $\eta^*$ ; Fig. 4(b)]. This behavior was consistent with the equivalent MW evolution; that is, both the modulus and the viscosity decreased significantly along the extruder, with a sudden decline around a length/diameter ratio ( $L/D$ ) of 10.

These data were used with the theoretical model to couple the chemical conversion with changes in the

TABLE  
Melting Temperatures ( $^{\circ}\text{C}$ ) at the Sampling Locations

IV

Trial	$L/D = 9$	$L/D = 10$	$L/D = 11$	$L/D = 16$	$L/D = 21$	$L/D = 29$
1	173	195	201	204	205	203
2	179	191	193	207	209	200
3	180	186	192	201	201	199
4	188	213	215	228	226	222

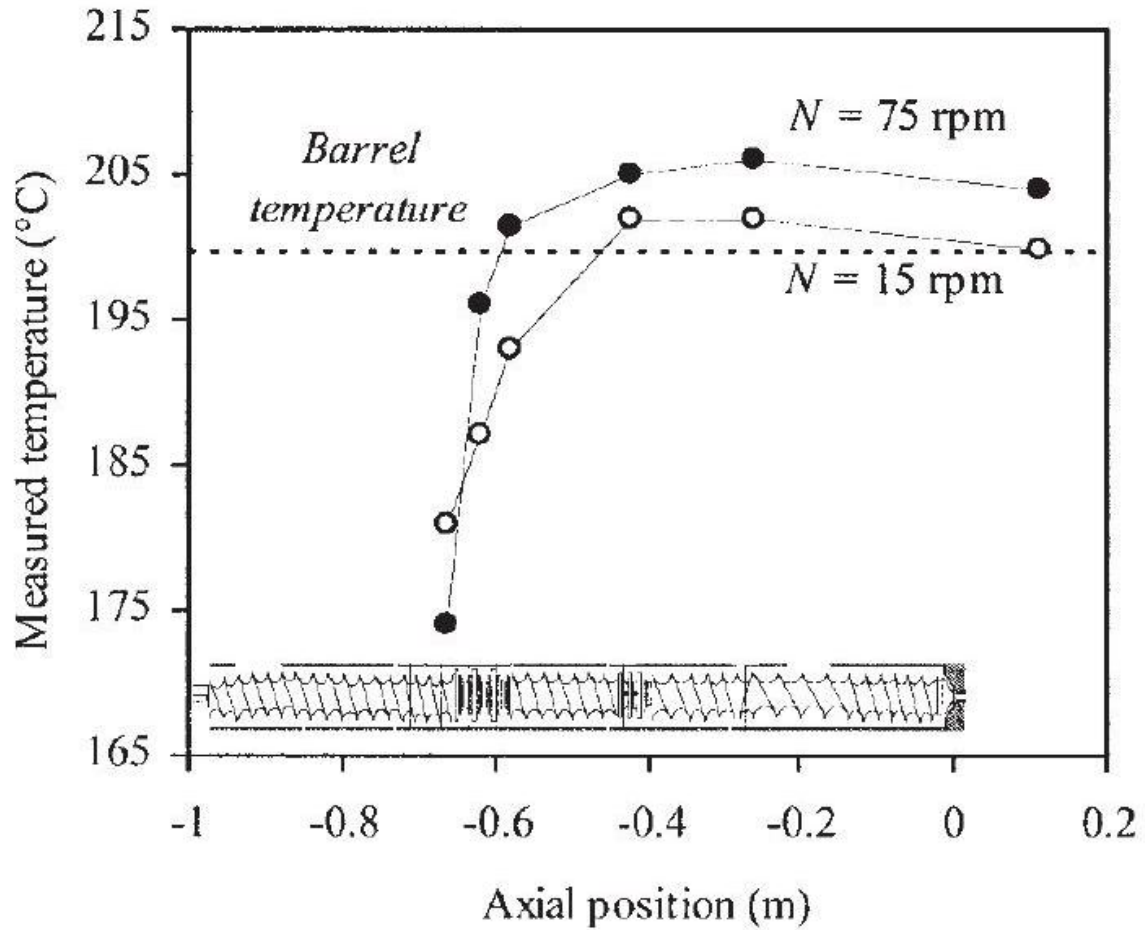


Figure 2 Changes in the temperature ( 200°C, 0.05phr ) measured along the screws: (○): 15 and (●) 75 rpm , where  $N$  is the screw rotation speed. viscosity. Such a nice rheology/chemistry correlation could also be used for online process control, if online oscillatory rheometry were available. <sup>17</sup>

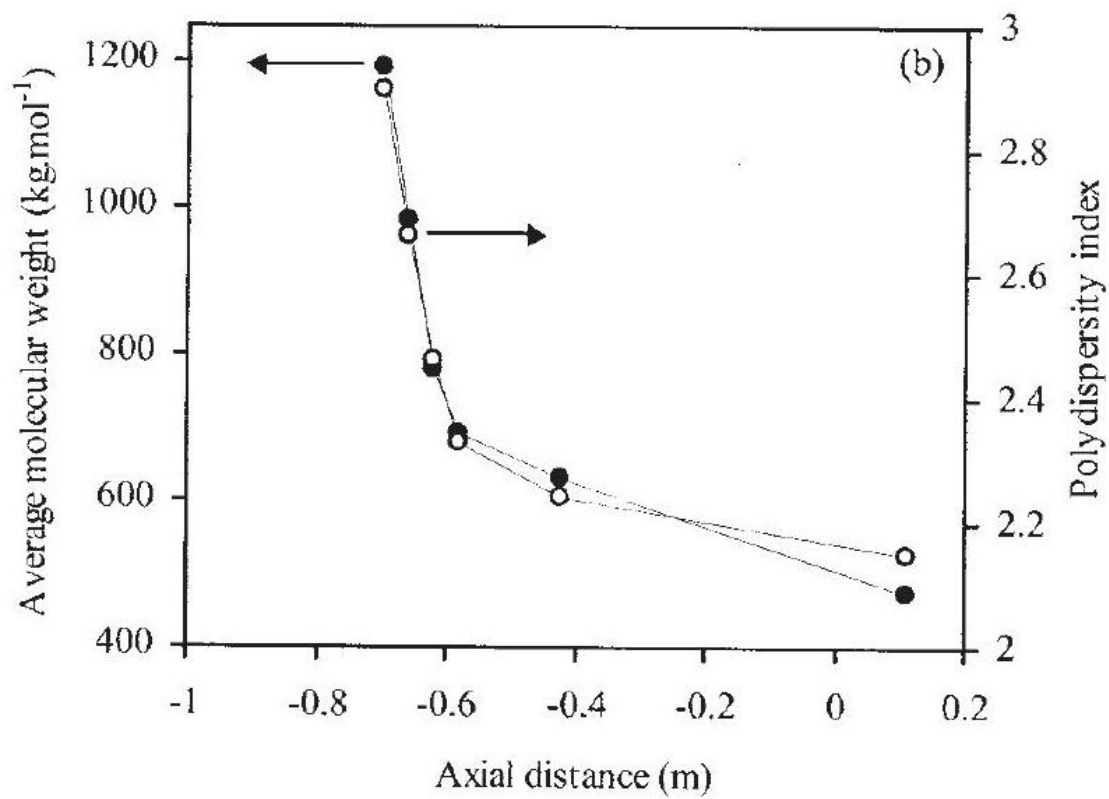
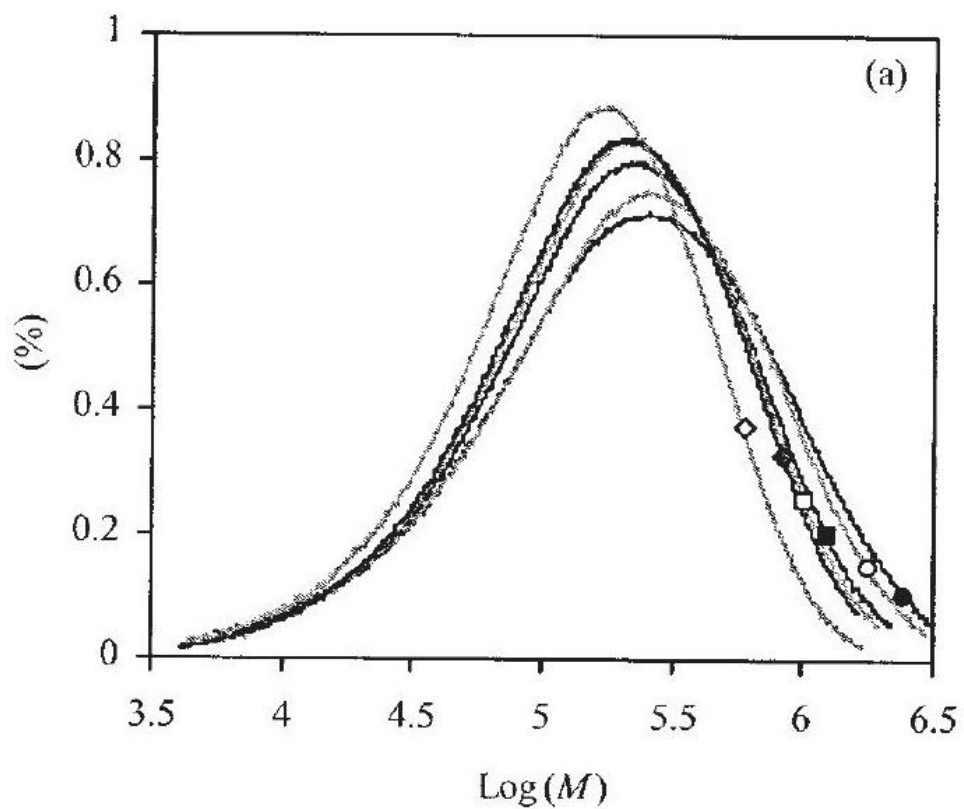


Figure 3 (a) Changes in MWD [(•)  $L/D = 0$ , (○)  $L/D = 9$ , (■)  $L/D = 10$ , (□)  $L/D = 11$ , (▸)  $L/D = 16$ , and (◇) extrudate] and (b) changes in (•) the average MW and (○) polydispersity index measured along the screws ( 75 rpm , 200°C, 0.05phr).

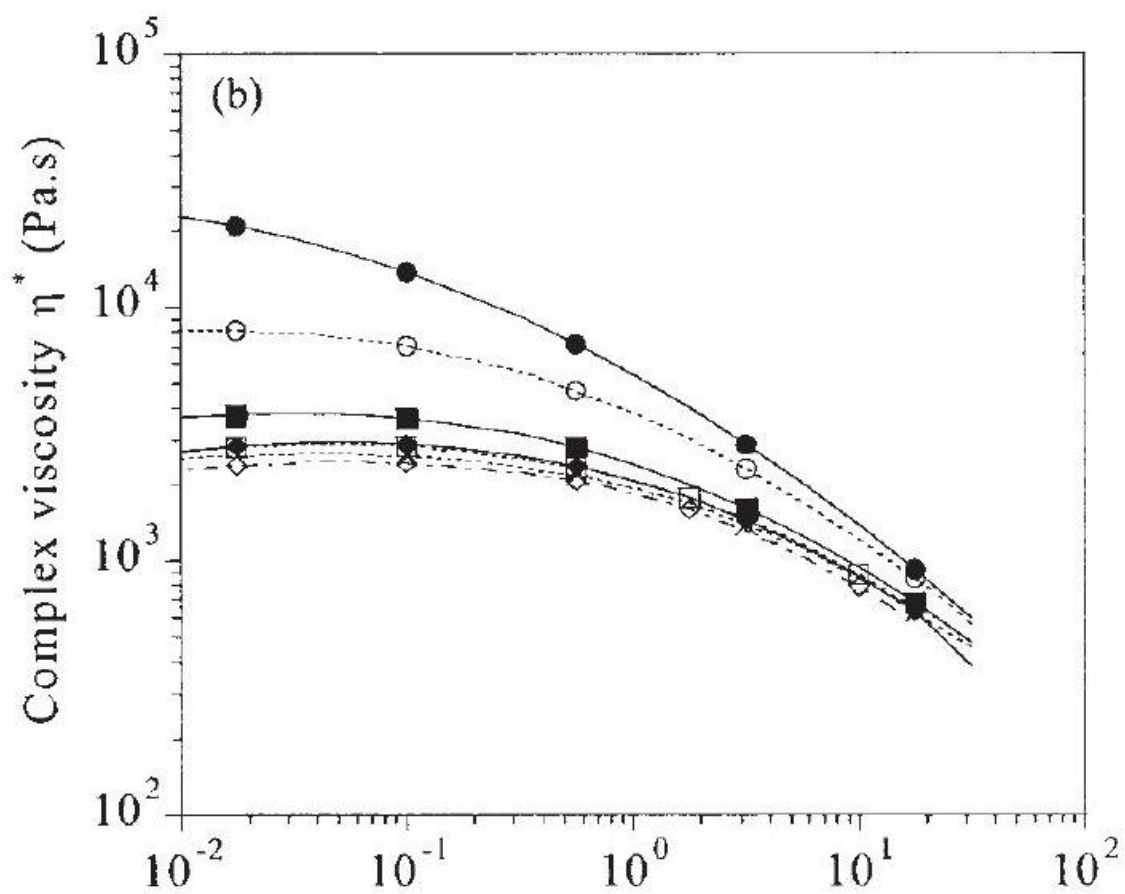
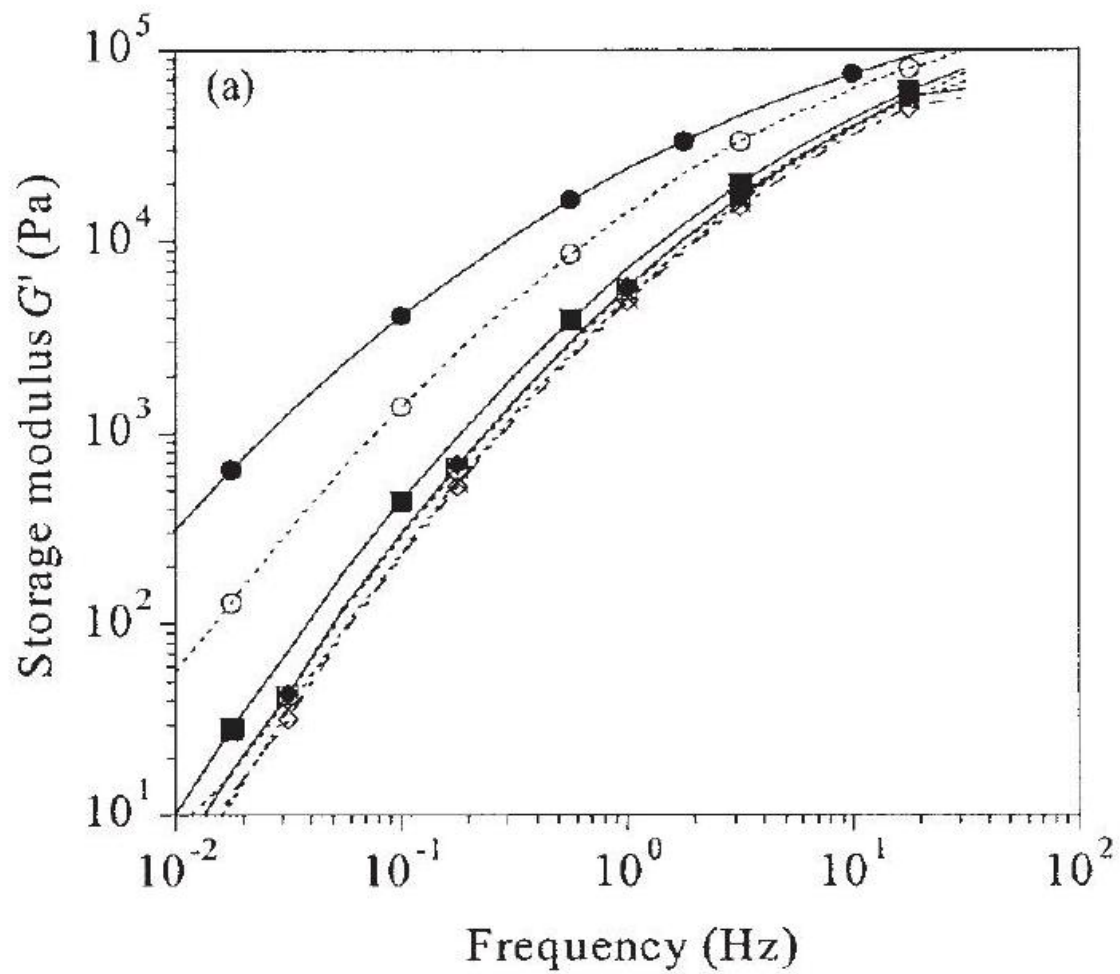


Figure 4 Evolution of (a)  $G'$  and (b)  $\eta^*$  along the screws (75 rpm, 200°C, 0.05phr): (·)  $L/D = 0$ , (○)  $L/D = 9$ , (□)  $L/D = 10$ , (◻)  $L/D = 11$ , (Δ)  $L/D = 16$ , ( )  $L/D = 21$ , and (×) extrudate (75rpm; 200°C; 0.05phr).

## Theoretical computations

Before checking the validity of the reactive model, we had to confirm whether the flow without the reaction was accurately described by the Ludovic software. Although the different processing conditions without peroxide were investigated systematically. Figure 5 provides an example of a comparison of the theoretical and experimental temperature profiles. The agreement was satisfactory, given the practical difficulty in measuring polymer melt flow temperatures. When the data were contrasted with those of Figure 2, we found that higher temperatures had been reached, as the virgin PP was much more viscous than the degraded PP. A global comparison embracing the different conditions and various sampling locations is presented in Figure 5(b). All the calculated temperatures (along the barrel and at the die exit) were within the  $\pm 5\%$  range of the experimental values, thus confirming the ability of Ludovic to calculate the flow conditions in a twinscrew extruder.

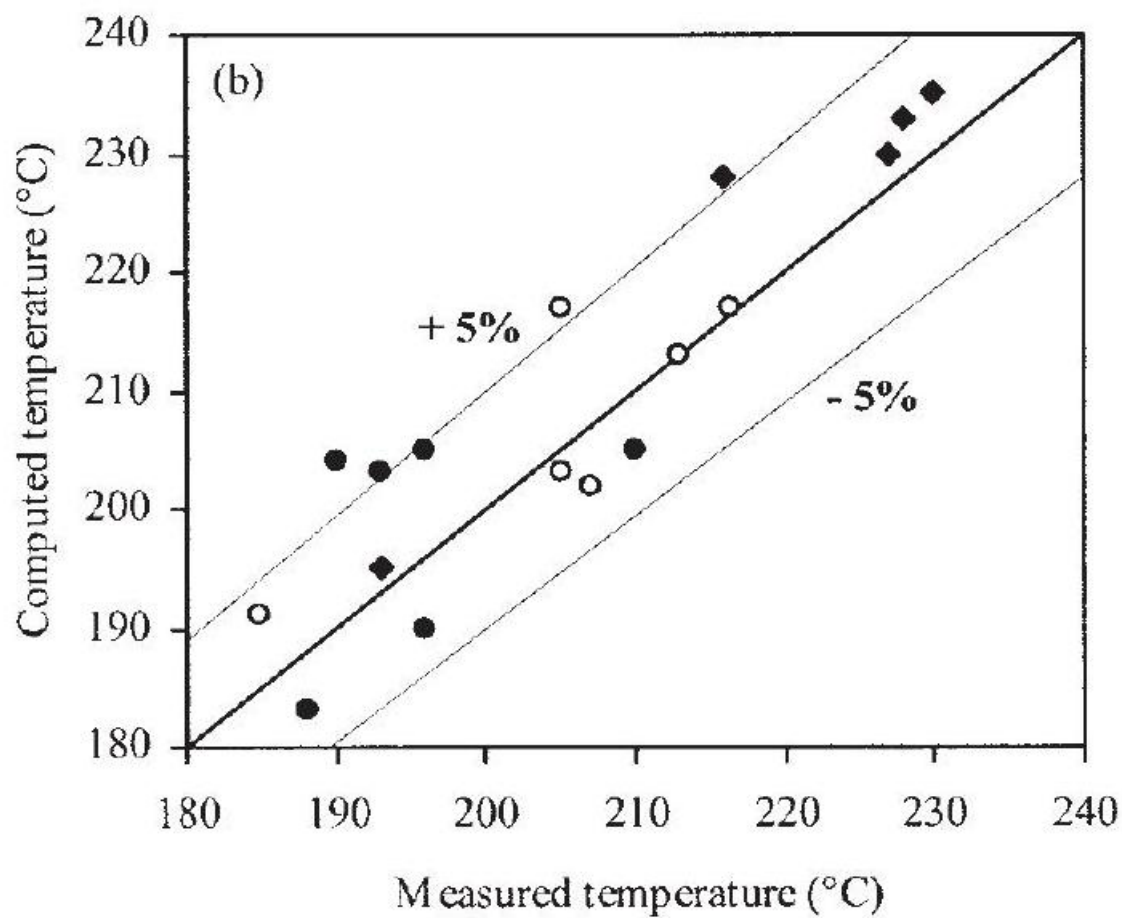
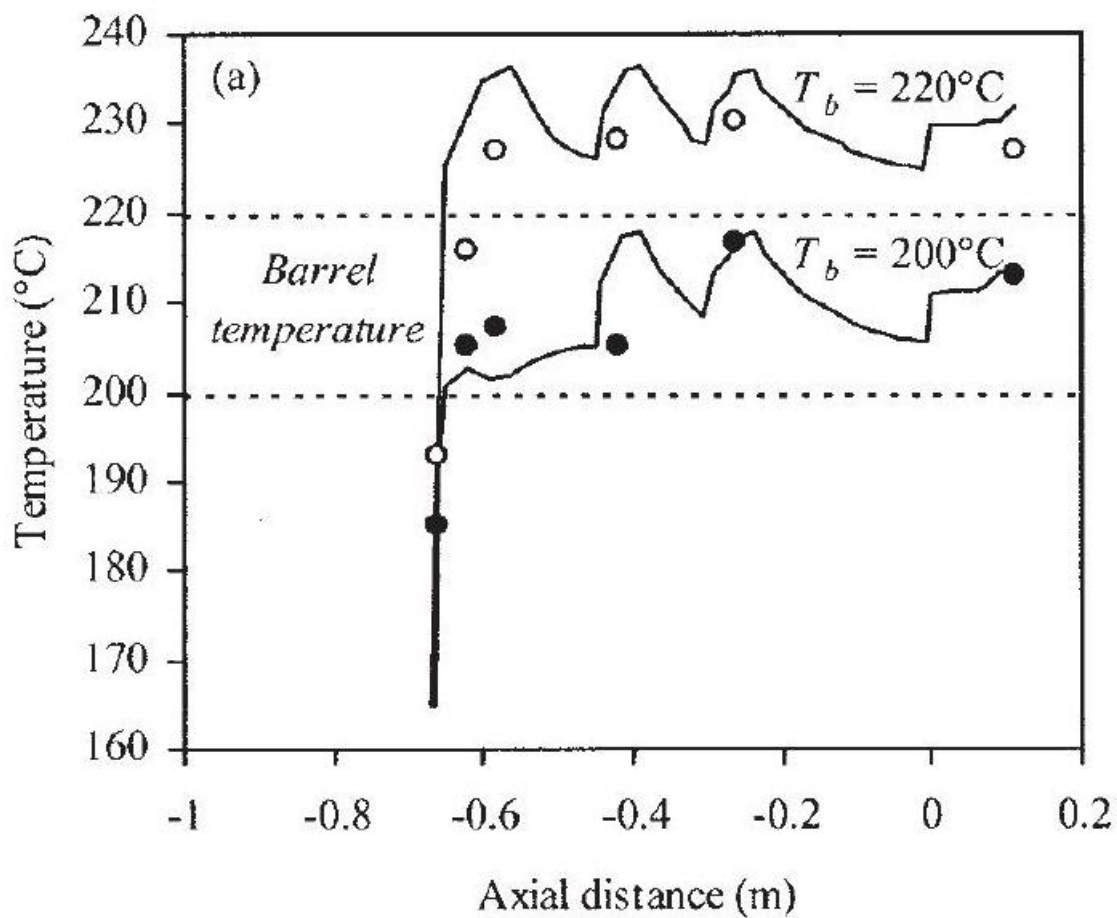


Figure 5 (a) Comparison of the computation and experimentation [75 rpm, (•) 200 and (○) 220°C ] without the reaction (temperature profiles) and (b) general comparison of all trials [(•)15rpm and 200°C, (○)75rpm and 200°C, and ( ) 75 rpm and 220°C;  $T_b$  = barrel temperature].

In the next step, the reaction kinetics were computed, coupled with viscosity changes. The only fitting parameter of the chemical model was the peroxide efficiency,  $f$ , which represents the ratio of free radicals leading to  $\beta$  scission to the total number of free radicals. Values between 0.6 and 1 are often used in the literature 9,18,19 for peroxide concentrations lower than 0.1%. Berzin et al. <sup>13</sup> showed that  $f$  could be considered a function of the peroxide concentration but independent of the processing conditions. Consequently, the correct value of the efficiency for trial 1 was estimated by the adjustment of  $f$  to obtain the experimental value of  $M_w$  at the die exit. The results for  $f = 0.365$  are shown in Figure 6, in which both the predicted and measured melting temperatures and MW evolution along the extruder axis are plotted. The agreement was quite reasonable, and this meant that the model was able to capture the main characteristics of this reactive extrusion process. This low value of  $f$  could be probably explained by the fact that the peroxide was preblended and fed together with the solid

PP pellets, instead of being injected into the molten PP. Therefore, the melting process plays an important role and, if peroxide starts to decompose before total melting, it can be lost for degradation, leading to poor efficiency.

Both the theoretical predictions previously discussed and the experimental points show that PP's MW decreased significantly in the first part of the extruder, that is, in the first mixing block during melting.

If we just consider the decomposition of the peroxide, the concentration at any time is given by

$$[I] = [I_0]\exp(-k_d t) \quad (1)$$

where  $[I_0]$  is the initial concentration,  $k_d$  is the rate constant, and  $t$  is the time.  $k_d$  follows the Arrhenius law:

$$k_d = A \exp\left(-\frac{\Delta E}{RT}\right) \quad (2)$$

The values of  $A$  and  $\Delta E/R$  were taken from the literature <sup>7-10</sup> and were equal to  $1.98 \times 10^{12}$  and 14,947 ,

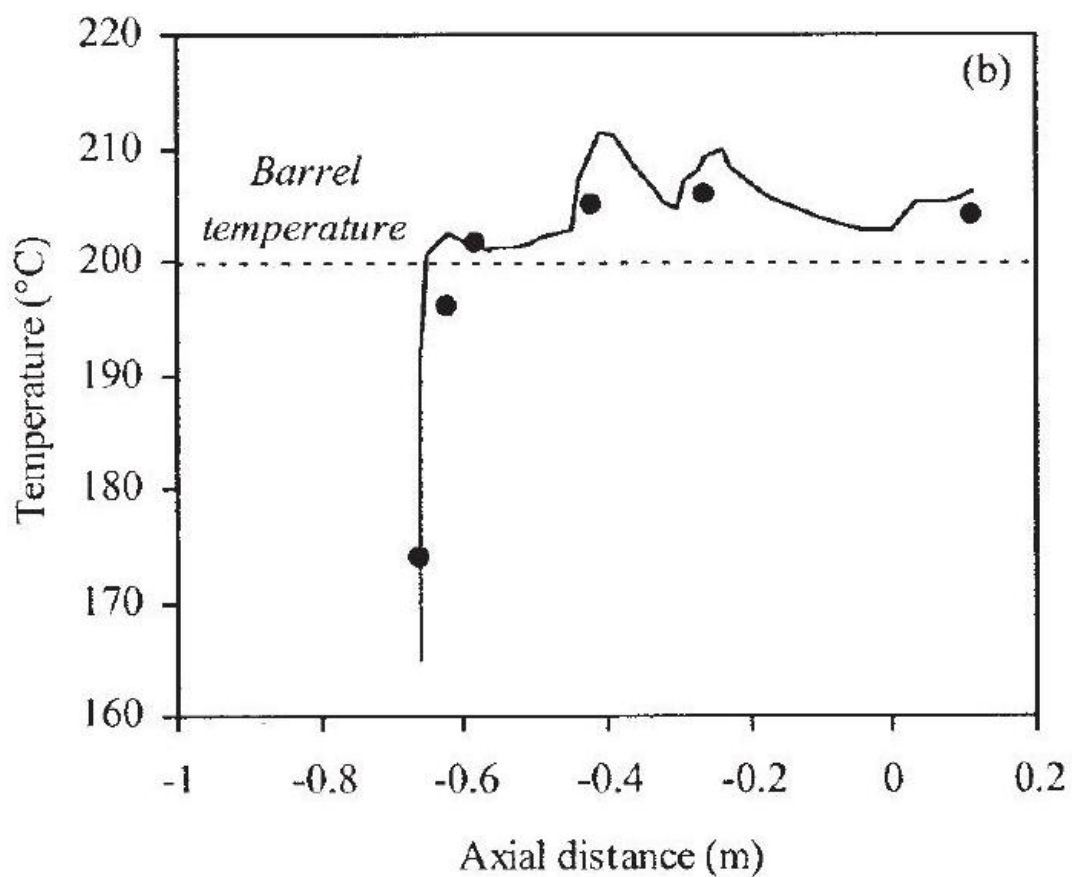
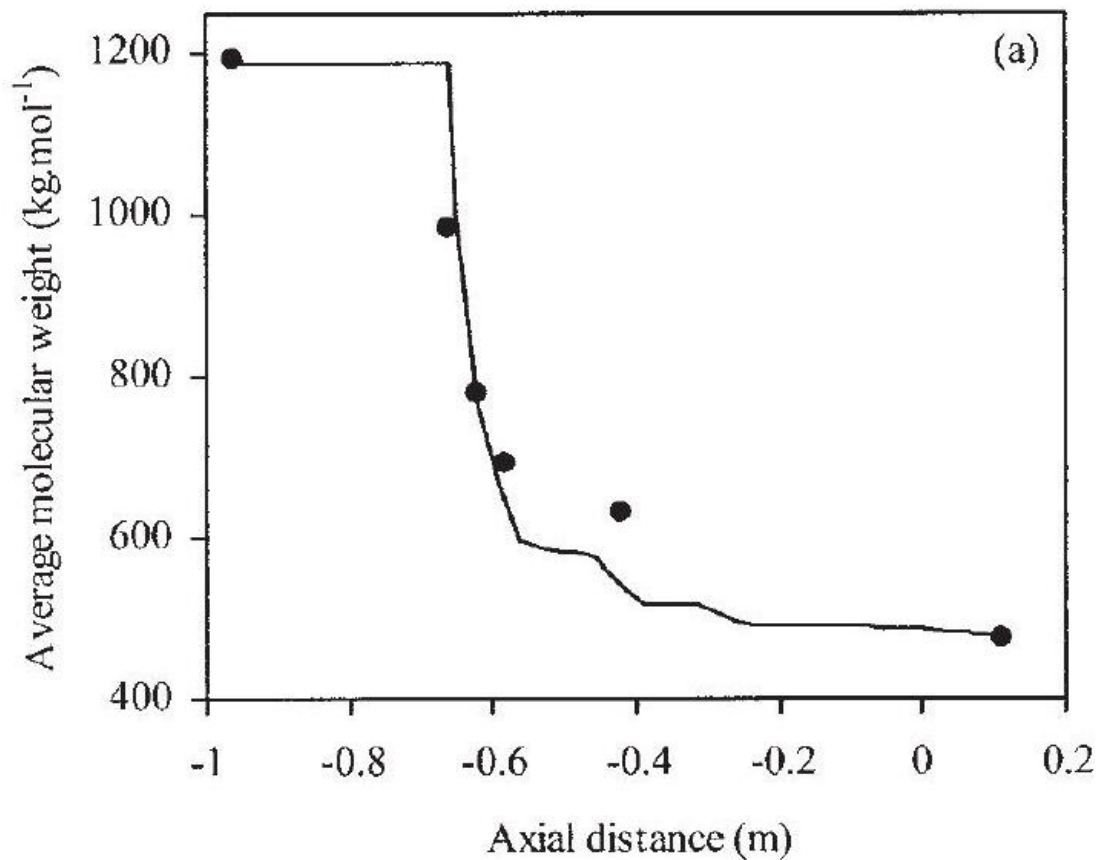


Figure 6 Comparison of the computation and (•) experimentation with the reaction (75rpm, 200°C, 0.05phr ): (a) average MW and (b) temperature.

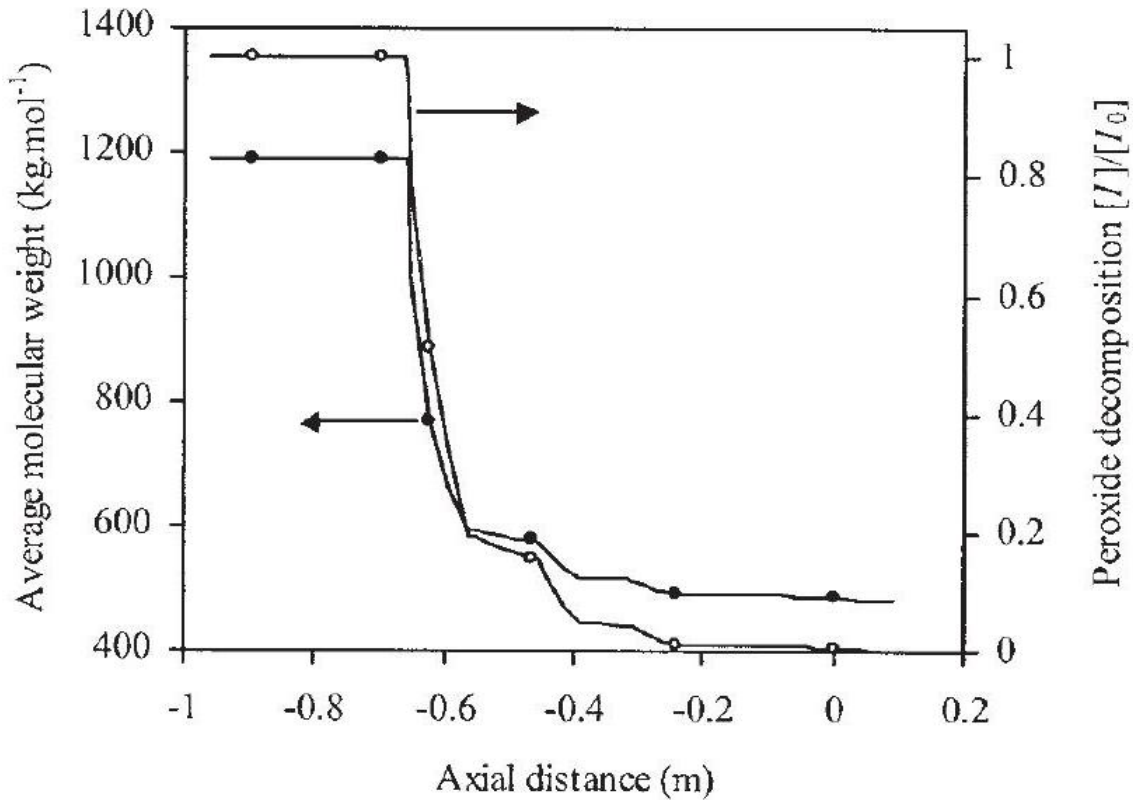


Figure 7 Comparison of the evolution along the screws (75 rpm, 200°C, 0.05phr) of (•) the computed average MW and (○) peroxide decomposition, respectively;  $\Delta E$  is the activation energy,  $R$  is the gas constant, and  $T$  is the absolute temperature. The residence time along the extruder was provided by Ludovic. Assuming that the temperature was equal to 200°C and that the peroxide decomposition started simultaneously with melting, we computed the change in the  $[I]/[I_0]$  ratio along the screws with eqs. (1) and (2). As shown in Figure 7, the MW behavior mirrored that of peroxide decomposition, confirming the previously reported correlation between the two. <sup>17</sup>

## Influence of the peroxide content

Figure 8 exhibits the evolution of the MW of PP samples processed under the same conditions, but with two different peroxide incorporation levels (0.05 and 0.1 phr ). The predictions were made under the assumption of the same  $f$  value. MW was progressively

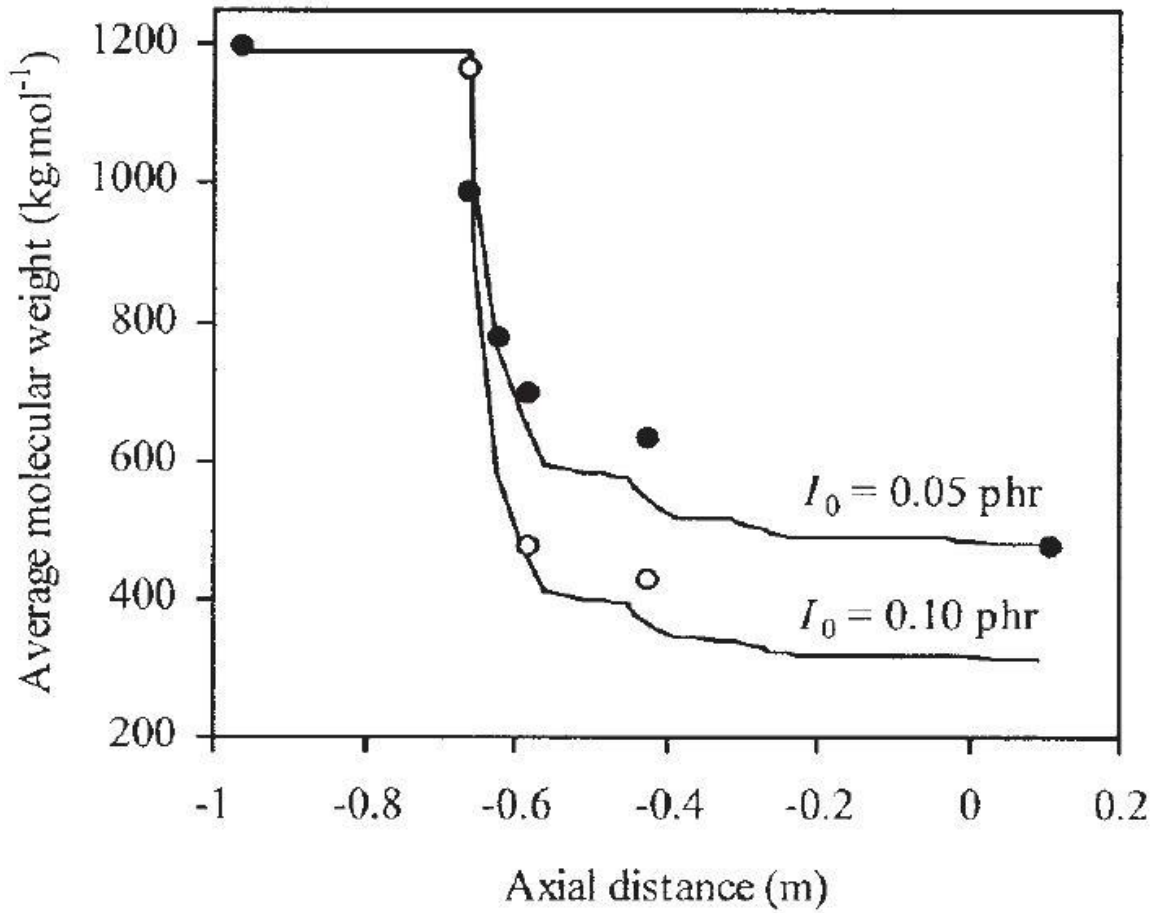


Figure 8 Comparison of the  $M_w$  values of the computation and experimentation ( 75rpm, 200°C ) for two levels of peroxide: (●)0.05 and (○)0.10phr.

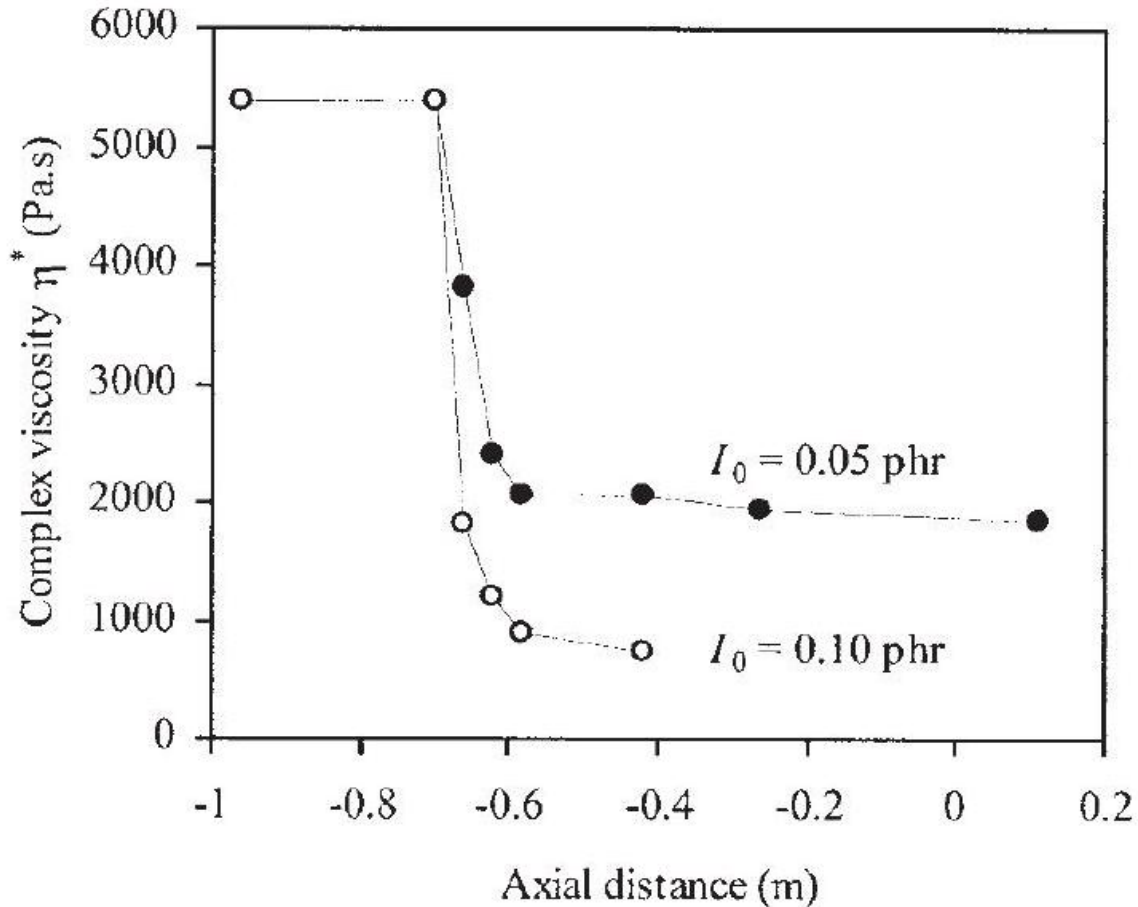


Figure 9 Changes in  $\eta^*$  at 1 Hz along the screws (75 rpm, 200°C) for two levels of peroxide: (●)0.05 and (○)0.10 phr. reduced because of chain scission taking place mainly upon the melting of PP (see also Table III for quantitative data). The higher the amount was of peroxide, the more significant the decline was in MW because of the generation of more free radicals, which promoted more chain scission. However, the degradation pattern was identical. The model was able to capture these features quite well.

As expected and shown in Figure 9, the rheological parameters emulated this performance; that is, with increasing peroxide content, the decrease in  $\eta^*$  was more dramatic but occurred at the same location, and an equivalent plateau was identified.

## Influence of the screw speed

Figure 10 illustrates the theoretical and experimental evolution of MW along the extruder when PP was modified with 0.05 phr peroxide at distinct screw speeds (15 and 75 rpm) and at a constant set barrel temperature (200°C). At the lower speed, the MW changes were less significant and probably slower, in light of the relative peroxide decomposition rate. The model predicted similar decays, but the final plateaus were correctly anticipated. However, the efficiency was decreased from 0.365 at 75 rpm to 0.265 at 15 rpm to match the final experimental value. This need was likely caused by the specific extrusion environment present at a very low screw speed, causing modifications in the melting

process with effects on the efficiency of the peroxide action. With an efficiency of 0.365, we would have obtained at the die exit a theoretical MW of 489,000 g/mol, in comparison with the experimental value of 567,500 g/mol.

The rheological parameters were less able to discriminate the global effect of the screw speed (Fig. 11). No significant differences in the rate of  $\eta^*$  drop-off could be identified.

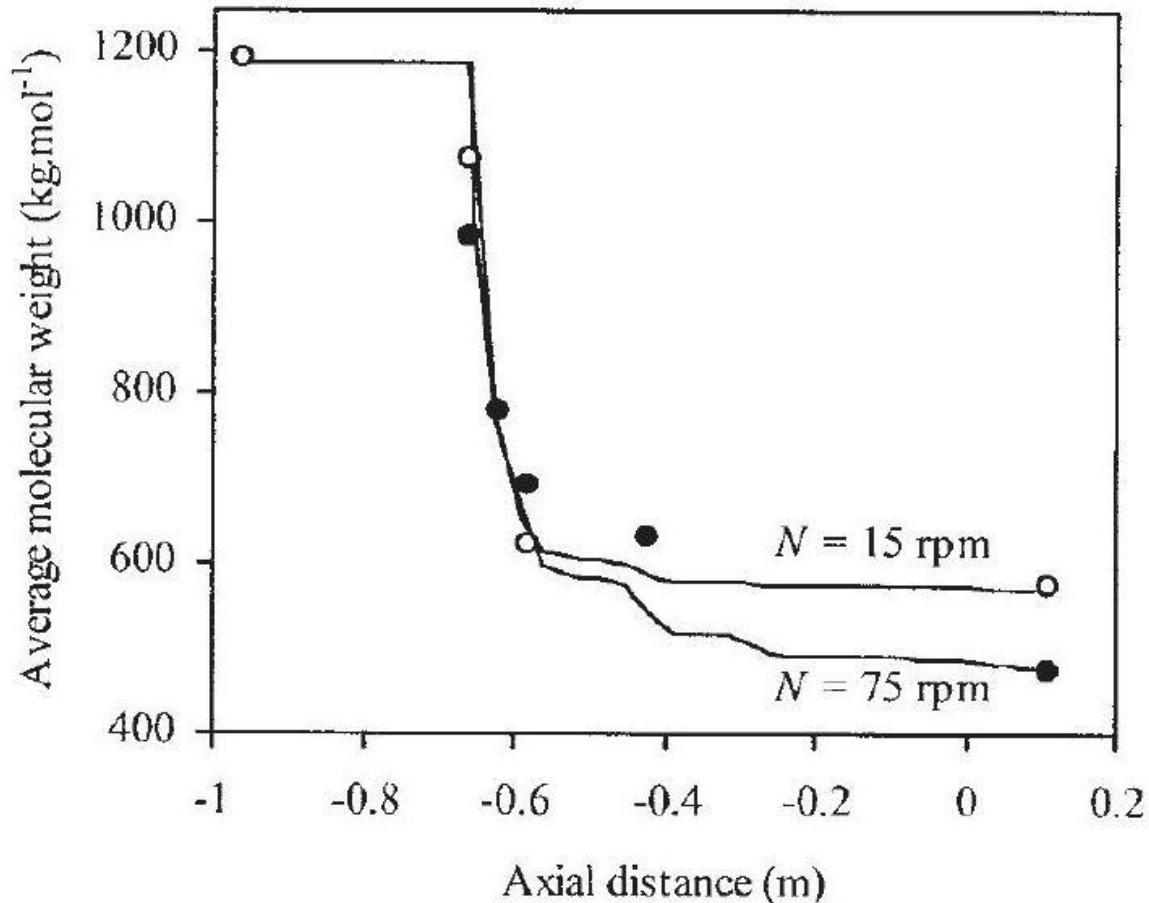


Figure 10 Comparison of the  $M_w$  values of the computation and experimentation (0.05phr, 200°C) at two screw speeds: (○)15 and (●)75rpm.  $N$  is the screw rotation speed.

## Influence of the barrel temperature

The effect of temperature on the degradation reaction for PP plus 0.05 phr DHBP is evident from an analysis of Figure 12 at extrusion temperatures of 200 and 220°C. The decrease in MW and the shift of the MWD curves were much less apparent in the later case. This could be explained by the faster decomposition of the peroxide at 220°C (at this temperature, the half-life of the peroxide was 1.2 s). Thus, probably most of the peroxide was decomposed before the polymer started to melt, and as a result, a very small amount of peroxide was used as an initiator of the degradation reaction. This also explained why the adjusted efficiency was now 0.106, that is, the lowest value of all experiments. Again, Figure 13 demonstrates that the change in MW was directly controlled by the peroxide

decomposition [computed with eqs. (1) and (2)]. Rheological measurements (Fig. 14) were in agreement with

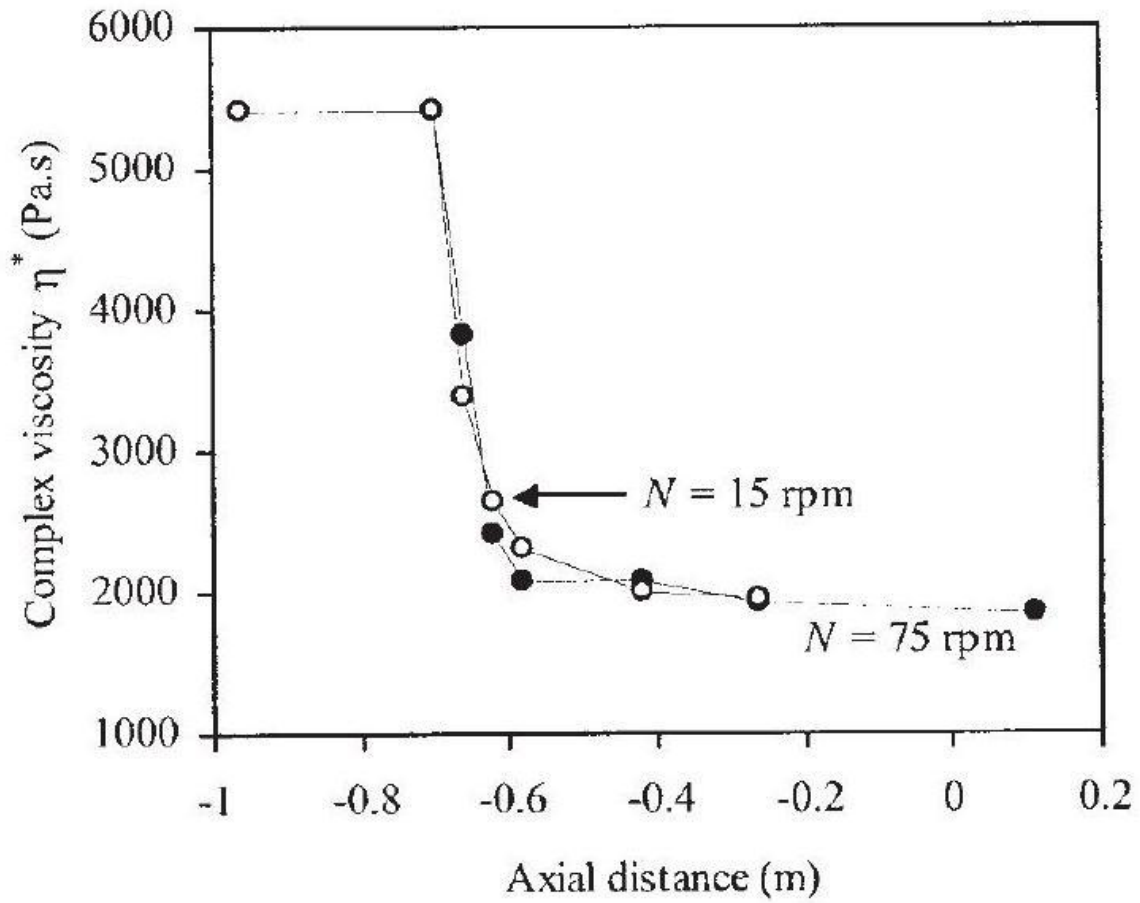


Figure 11 Change in  $\eta^*$  at 1 Hz along the screws ( 0.05 phr , 200°C ) at two screw speeds: (○) 15 and (●) 75 rpm.

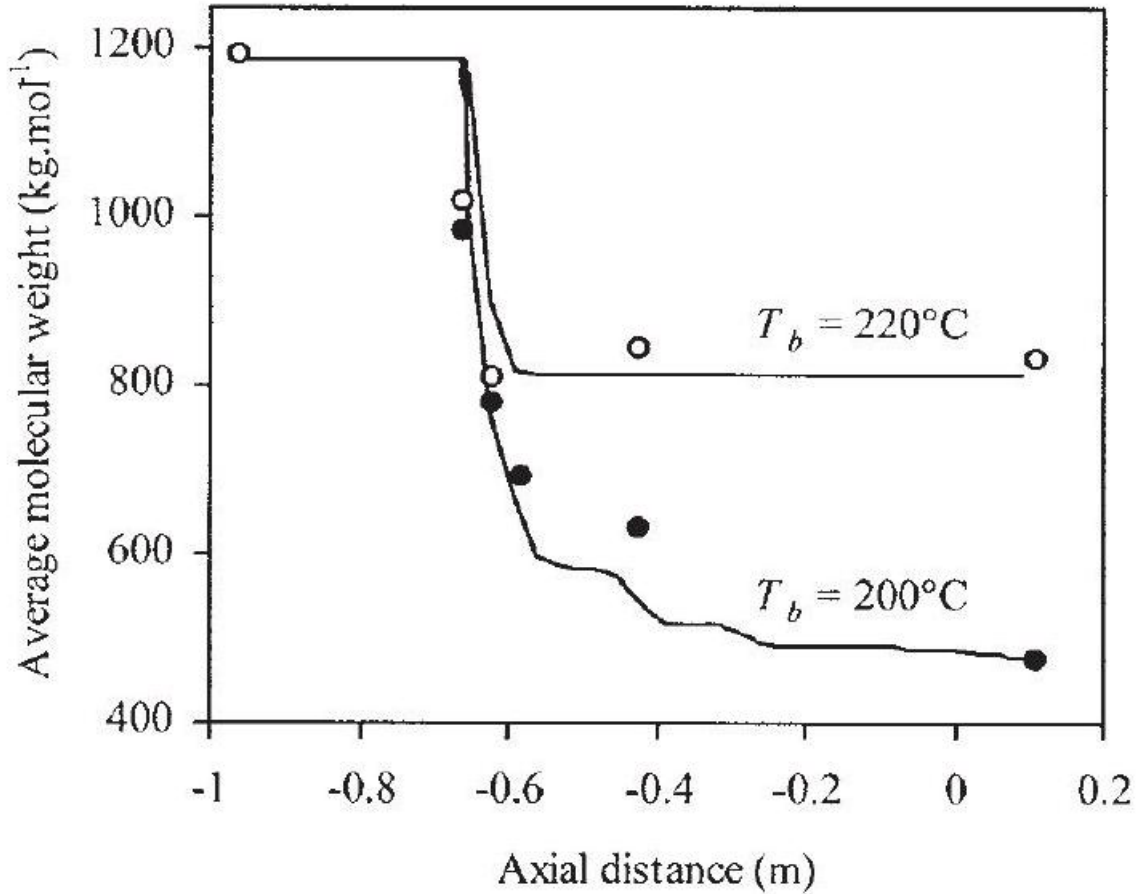


Figure 12 Comparison of the  $M_w$  values of the computation and experimentation ( 75rpm, 0.05phr ) at two barrel temperatures (  $T_b$ 's ): (  $\cdot$  ) 200 and (  $\circ$  ) 220°C. these results, which exhibited a smaller decrease in  $\eta^*$  at a higher temperature.

## CONCLUSIONS

An experimental study using sampling devices along the screw profile validated a previously developed theoretical model of peroxide-induced degradation of PP in twin-screw extruders. Degradation started upon melting of the polymer and proceeded rapidly, inducing a rapid drop in the MW and viscosity. The evolution of the MW was mimicked by the kinetics of the peroxide decomposition. In all cases, the theoretical model was able to capture the main process features and describes accurately the evolution of the material properties, once the efficiency of the peroxide was determined. In comparison with previous studies, we found here very low values of efficiency, explained by

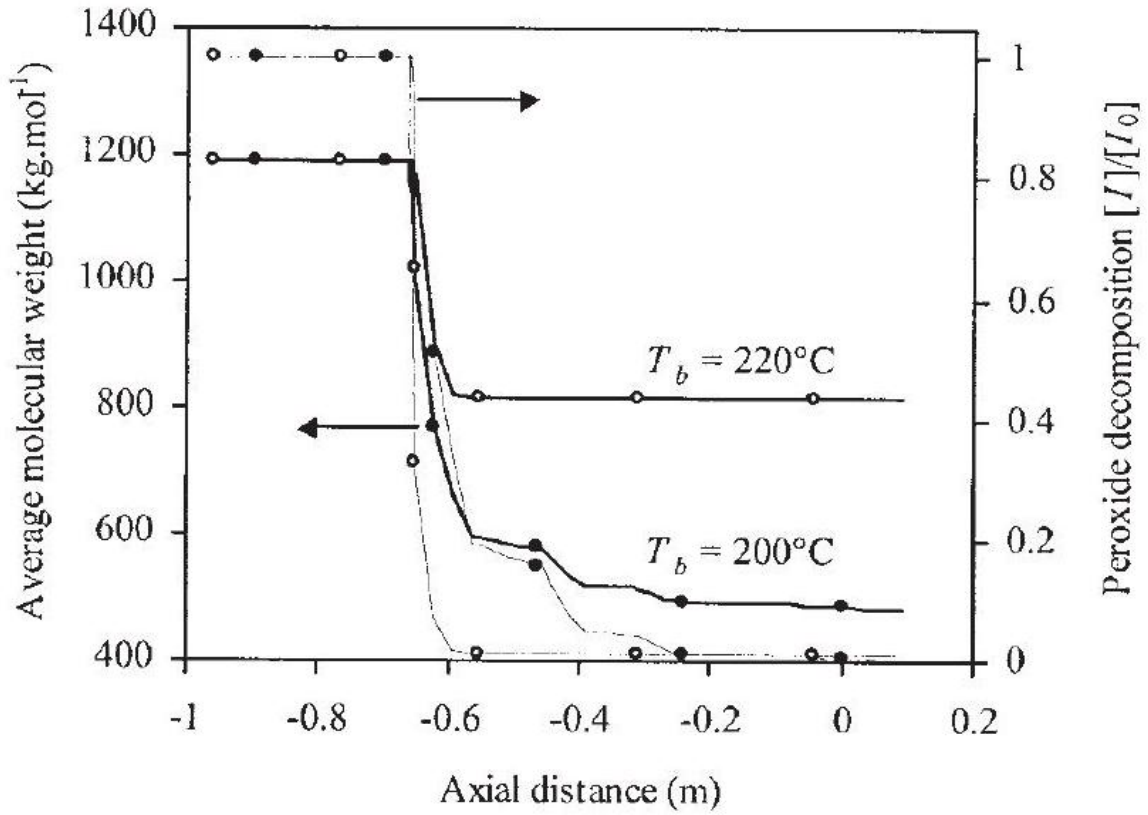


Figure 13 Comparison of the evolution along the screws ( 75rpm, 0.05phr ) of the computed average MW and peroxide decomposition for two barrel temperatures (  $T_b$  's ): 200 and 220°C.

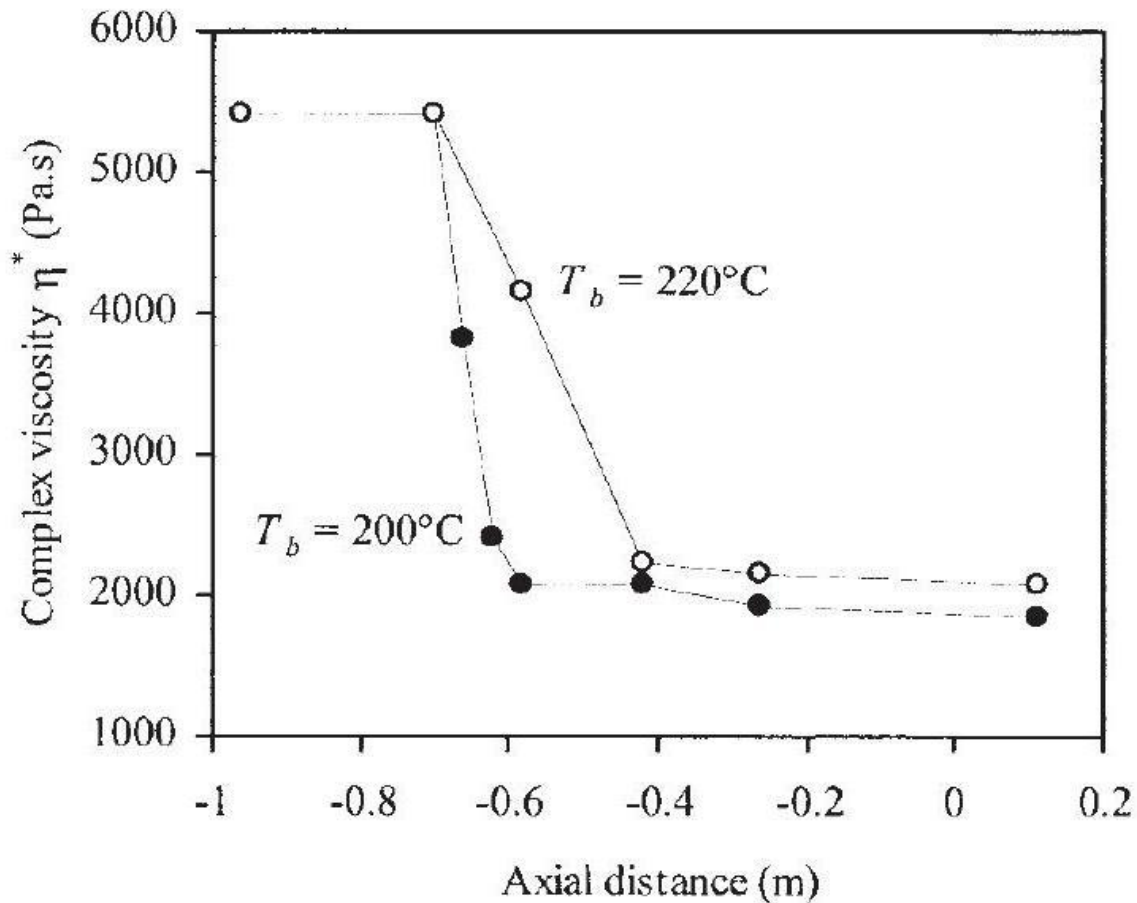


Figure 14 Changes in  $\eta^*$  at 1 Hz along the screws ( 75 rpm , 0.05 phr ) for two barrel temperatures (  $T_b$ 's ): (  $\bullet$  ) 200 and (  $\circ$  ) 220°C. the fact that the peroxide was introduced as a solid into the hopper, instead of being injected into the molten polymer.

## References

1. Casale, A.; Porter, R. Polymer Stress Reactions; Academic: New York, 1978.
2. Xanthos, M. Reactive Extrusion; Hanser: New York, 1992.
3. Al-Malaika, S. Reactive Modifiers for Polymers; Blackie Academic: London, 1997.
4. Machado, A. V.; Covas, J. A.; van Duin, M. J Appl Polym Sci 2001, 81, 58.
5. Berzin, F.; Vergnes, B.; Delamare, L. J Appl Polym Sci 2001, 80, 1243.
6. Wiyatno, W.; Chen, Z. R.; Liu, Y. X.; Waymouth, R. M.; Krukonis, V.; Brennan, K. Macromolecules 2004, 37, 701.
7. Suwanda, D.; Lew, R.; Balke, T. J Appl Polym Sci 1988, 35, 1019.
8. Suwanda, D.; Lew, R.; Balke, T. J Appl Polym Sci 1988, 35, 1033.
9. Tzoganakis, C.; Vlachopoulos, J.; Hamielec, A. E. Polym Eng Sci 1988, 28, 170.
10. Tzoganakis, C.; Tang, Y.; Vlachopoulos, J. Polym Plast Technol Eng 1989, 28, 319.

11. Pabedinskas, A.; Cluett, W.; Balke, S. *Polym Eng Sci* 1994, 34, 993.
12. Kim, B.; White, J. L. *Polym Eng Sci* 1997, 37, 576.
13. Berzin, F.; Vergnes, B.; Dufossé, P.; Delamare, L. *Polym Eng Sci* 2000, 40, 344.
14. Machado, A. V.; Covas, J. A.; van Duin, M. *J Appl Polym Sci* 1999, 71, 135.
15. Vergnes, B.; Della Valle, G.; Delamare, L. *Polym Eng Sci* 1998, 38, 1781.
16. Vergnes, B.; Souveton, G.; Delacour, M. L.; Ainsler, A. *Int Polym Proc* 2001, 16, 351.
17. Machado, A. V.; Maia, J. M.; Canevarolo, S. V.; Covas, J. A. *J Appl Polym Sci* 2004, 91, 2711.
18. Krell, M. J.; Brandolin, A.; Vallés, E. M. *Polym React Eng* 1994, 2, 398.
19. Ryu, R. H.; Gogos, C. G.; Xanthos, X. *Adv Polym Technol* 1992, 11, 121.

---

$Q = 2.3$  kg/h, where  $Q$  is the feed rate.